

Viatcheslav S. LOVEIKIN ¹, Yuriy O. ROMASEVYCH ¹,
Andriy V. LOVEIKIN ², Mykola M. KOROBKO ¹

Optimization of the trolley mechanism acceleration during tower crane steady slewing

Received 3 October 2021, Revised 31 March 2022, Accepted 4 April 2022, Published online 22 August 2022

Keywords: trolley, optimization, movement, criteria, crane

The article describes optimization of the process of acceleration of the tower crane trolley movement mechanism during the steady mode of the slewing mechanism. A mathematical model of the boom system of the tower crane was used for the optimization of the trolley movement. The model was reduced to a sixth-order linear differential equation with constant coefficients, which represents the relationships between the drive torque and the coordinate of the load and its time derivatives. Non-dimensional complex criterion (objective function), which takes into account the drive torque and its rate of change in time during the transient process, was developed to optimize the mode of the trolley movement mechanism. Based on that, a variational problem was formulated and solved in an analytical form in which root-mean-square (RMS) values of the quantiles were applied. A complex optimal mode of acceleration of the trolley movement mechanism was obtained and compared with the modes optimized based on different criteria. Advantages and disadvantages of the solutions were discussed based on the analysis of the obtained optimal modes of motion. The analysis revealed low- and high-frequency elements oscillations of the trolley movement mechanism during the transient processes. The conditions for their elimination were formulated.

✉ Yuriy O. Romasevych, e-mail: romasevichyuriy@ukr.net

¹National University of Life and Environmental Sciences of Ukraine, Kyiv, Ukraine. ORCIDs: V.S.L.: 0000-0003-4259-3900; Y.O.R.: 0000-0001-5069-5929; M.M.K.: 0000-0002-2602-4225

²Taras Shevchenko National University of Kyiv, Kyiv, Ukraine. ORCID (A.V.L.) 0000-0002-7988-8350



© 2022. The Author(s). This is an open-access article distributed under the terms of the Creative Commons Attribution (CC-BY 4.0, <https://creativecommons.org/licenses/by/4.0/>), which permits use, distribution, and reproduction in any medium, provided that the author and source are cited.

1. Introduction

In order to increase the capacity of a tower crane, several of its mechanisms often operate jointly. An example of such a joint operation is the movement of the load trolley combined with the movement of slewing mechanisms of the crane. In this case, there appear additional dynamical loads in elements of mechanisms and in the structure of the crane. These loads can be especially dangerous when one of the mechanisms is in the transient process (starting or braking). The loads may cause low- and high-frequency oscillations in the elements of a crane mechanism, which, in turn, lead to a decrease in the crane reliability and increase the energy losses in the crane mechanisms.

A significant number of scientific works have been dedicated to the dynamic processes during the operation of crane mechanisms. The dynamics of the hoisting and the trolley movement mechanisms for different types of cranes was studied in [1]. In this work, the load pendulum oscillations were described and investigated. In order to eliminate them, one developed controllers based on the Lyapunov techniques and LaSalle's invariance theorem [2, 3]. Other Lyapunov-based approach allowed for creating a closed-loop control system, which takes into account actuator constraints [4]. Experimental studies presented in this work support the theoretical basis of the research.

In addition to the pendulum oscillations, a twisting of a load exists in practice. Investigations on this problem and means for reduction were presented as well [5].

The above-mentioned investigations exploit the idea of double-pendulum oscillations (hook and load). Elimination of the load pendulum oscillations can be achieved with the application of soft computing approaches (artificial neural network and fuzzy-logic) [6, 7]. A similar goal was set in the work [8], where PID-controllers (in different forms) were used to solve the problem.

All of these approaches are effective. However, they do not comply with the idea of optimal control. There are many scientific investigations [9–13], where optimal control problems were formulated and solved in different ways.

In the work [9], a crane-trolley-load dynamical system is modeled with coupled ordinary-partial differential equations. They were exploited in an optimal control problem, and the authors provided a solution to the problem in a numerical form. In order to reduce the load pendulum (low-frequency) oscillations, the problem of slewing mechanism optimization was solved [10]. All the obtained results have been numerical and the changes in parameters of the system lead to the need for recalculation of the optimal control law according to the new values of parameters (previously calculated law may be used as a first iteration to the new optimal control law). In the scientific work [11], a model of a tower crane is presented as a system of four nonlinear differential equations. In the formulation of optimal control problem, the authors imposed constraints on velocities and accelerations of the trolley movement and the tower slewing. The obtained quasi-optimal trajectory planning of the jib/trolley movement was validated via lab experiments. Similar results (in

terms of minimization criterion) were achieved in the article [12]. However, acceleration constraints were imposed on the load movement, as well. Experimental and theoretical data from these two investigations are close to each other. An advanced closed-loop control of three mechanisms of a tower crane was developed in the article [13]. The authors of this work applied the sequential distributed model predictive control (MPC) to jib, trolley, and hoist movements, and verified it via simulation and experimentally.

Almost all of the analyzed works involve lab installations and/or their parameters in calculations. This may lead to difficulties in practical implementation. On the other hand, in spite of the great variety of the closed-loop controls for different tower crane mechanisms, in many cases, the open-loop strategy may lead to desired results (as far as pendulum oscillations elimination and minimization criteria are concerned).

In the present work, we focus on a particular (however, very common in practice) case: steady slewing of the tower crane and optimal open-loop control of the trolley movement by a complex integral minimization criterion. Also, in the calculations, we use the parameters of a real tower crane.

2. Optimization problem statement

A three-mass dynamic model of the tower crane boom is used in the calculations (Fig. 1).

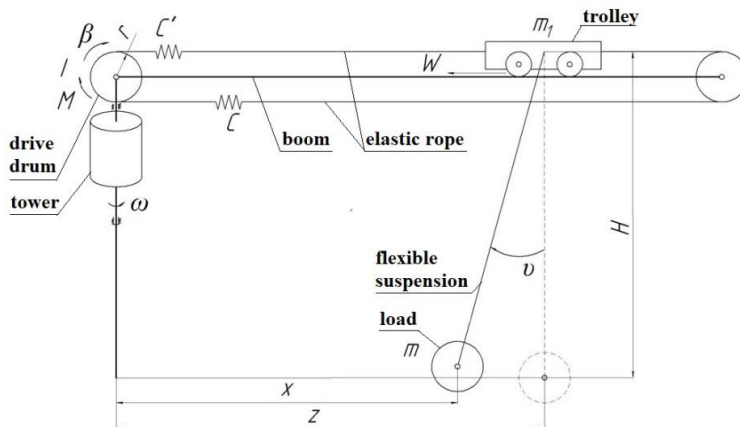


Fig. 1. Dynamic model of the trolley movement mechanism at the steady crane slewing

In the presented dynamical model, the load is attached to the center of mass of the trolley with a cable of constant length H . The trolley is connected with a drive drum by means of an elastic rope whose stiffness coefficient equals C or C' depending on the direction of the trolley motion. In further calculations, we consider the case of the trolley's backwards movement with respect to the tower.

In the case when the trolley moves towards the tower, the value C' is applied. The value of the stiffness coefficient influences the optimal law of the system motion. The load deviates from the vertical (in the plane of the trolley movement) by an angle ν . The elements of the drive mechanism, the drive drum, the trolley, and the load are assumed to be perfectly rigid bodies. The slewing motion of the boom system occurs at a constant angular velocity ω .

The linear horizontal coordinates of the trolley z and the load x , as well as the angular coordinate of the drive drum rotation β , are the generalized coordinates of the dynamic model.

The system of three second-order linear differential equations corresponds to the dynamic model (Fig. 1):

$$\begin{aligned}
 I\ddot{\beta} &= M - Cr(\beta r - z), \\
 m_1\ddot{z} - m_1\omega^2 z &= C(\beta r - z) - \frac{mg}{H}(z - x) - W, \\
 m\ddot{x} - m\omega^2 x &= \frac{mg}{H}(z - x),
 \end{aligned} \tag{1}$$

where I and M – the moment of inertia of the rotating elements of the trolley movement mechanism and the drive torque, respectively (they are reduced to the axis of the drum rotation); r – the radius of the drive drum; m_1 , m – masses of the trolley and the load, respectively; W – the force of static resistance to the trolley movement, which is accepted as a constant value (the force W is caused by the Coulomb friction); g – free-fall acceleration.

Let's express the linear coordinate z and the angular coordinate of the drum β via the coordinate x and its time derivatives:

$$z = \left(1 - \frac{H}{g}\omega^2\right)x + \frac{H}{g}\ddot{x}, \tag{2}$$

$$\begin{aligned}
 \beta &= \frac{1}{Cr} \left\{ \left[(C - m_1\omega^2) \left(1 - \frac{H}{g}\omega^2\right) - m\omega^2 \right] x \right. \\
 &\quad \left. + \left[(C - 2m_1\omega^2) \frac{H}{g} + m_1 + m \right] \ddot{x} + m_1 \frac{H}{g} \overset{IV}{x} + W \right\}.
 \end{aligned} \tag{3}$$

Taking into account expressions (2) and (3), the system (1) may be reduced to a linear differential equation of 6-th order, which describes the relationship between the drive torque and the load position x and its time derivatives:

$$M = a_0 + a_1x + a_2\ddot{x} + a_3 \overset{IV}{x} + a_4 \overset{VI}{x}, \tag{4}$$

where

$$\begin{aligned}
 a_0 &= Wr, \quad a_1 = - \left[m + m_1 \left(1 - \frac{H}{g} \omega^2 \right) \right] \omega^2 r, \\
 a_2 &= \frac{I}{Cr} \left[\left(C - m_1 \omega^2 \right) \left(1 - \frac{H}{g} \omega^2 \right) - m \omega^2 \right] + \left[m + m_1 \left(1 - 2 \frac{H}{g} \omega^2 \right) \right] r, \\
 a_3 &= \frac{I}{Cr} \left[\left(C - m_1 \omega^2 \right) \frac{H}{g} + m_1 \left(1 - \frac{H}{g} \omega^2 \right) + m \right] + m_1 \frac{H}{g} r, \\
 a_4 &= \frac{m_1 IH}{Crg}, \quad a_{0,1,2,3,4} = \text{const.}
 \end{aligned} \tag{5}$$

In the previously conducted dynamic analysis of the joint motion of the trolley movement and crane slewing mechanisms, it was found that during the acceleration process there appear significant force and energy overloads in the elements of the mechanisms and the metal structure of the crane. They depend on the drive torque. In addition, there are low- and high-frequency oscillations of the elements of mechanisms that depend on the drive torque, as well [12]. Therefore, there is a need to optimize the modes of motion of the trolley movement mechanism during steady slewing of the crane.

The previously conducted researches involved complex criteria. They showed that each of the criteria improve some properties of the mechanisms and make others worse. Thus, there is a problem of a reasonable compromise in different optimal modes of motion.

In this regard, it was suggested to optimize the mode of the trolley movement mechanism by a complex non-dimensional dynamic criterion, which takes into account the drive torque and its rate of change. It may be presented as follows:

$$K_1 = \left(t_1^{-1} \int_0^{t_1} \delta k \left(\frac{M}{M_{\text{RMS.min}}} \right)^2 + (1 - \delta) \left(\frac{\dot{M}}{\dot{M}_{\text{RMS.min}}} \right)^2 dt \right)^{1/2} \rightarrow \min, \tag{6}$$

where t – time; t_1 – duration of the trolley mechanism movement acceleration; $M_{\text{RMS.min}}$ – minimum RMS value of the function M during acceleration; \dot{M} – time derivative of the function M ; $\dot{M}_{\text{RMS.min}}$ – minimum RMS value of the function \dot{M} during acceleration; k – coefficient which reduces numerical values of components of the complex criterion (6) to the same degree; δ – non-dimensional weight coefficient, which varies from 0 to 1 and reflects the importance of the drive torque minimization.

In the frame of this investigation, there aren't any constraints in the problem statement.

3. Optimization problem solving

In order to determine the value $M_{\text{RMS.min}}$ in the complex criterion it is necessary to solve the following variational problem: to determine the motion law $x = x(t)$, $0 \leq t \leq t_1$, which minimizes the functional:

$$M_{\text{RMS.min}} = M_{\text{RMS}}^{(0)} = \left(t_1^{-1} \int_0^{t_1} M^2 dt \right)^{1/2} \rightarrow \min, \quad (7)$$

if the boundary conditions are met:

$$\begin{aligned} t = 0: \quad & x = x_0, \quad \dot{x} = 0, \quad \ddot{x} = x_0 \omega^2, \quad \overset{IV}{x} = 0, \quad \overset{V}{x} = x_0 \omega^4, \quad \overset{VI}{x} = 0, \\ t = t_1: \quad & x = x_0 + \frac{Vt_1}{2}, \quad \dot{x} = V, \quad \ddot{x} = \left(x_0 + \frac{Vt_1}{2} \right) \omega^2, \quad \overset{IV}{x} = 0, \\ & \overset{IV}{x} = \left(x_0 + \frac{Vt_1}{2} \right) \omega^4, \quad \overset{V}{x} = V \omega^4, \end{aligned} \quad (8)$$

where x_0 – the initial value of the load coordinate; V – steady velocity of the load. These boundary conditions reflect the necessary conditions for load oscillation elimination: the initial values of x and its derivatives correspond to the rest state of the load and the trolley; the final conditions mean that the positions and velocities of the load and the trolley are the same. That provides the elimination of the load oscillation at the end of the controlled start. The coordinate z and its derivatives are not represented in (8). They correspond to the 3-rd and higher derivatives of x , which are expressed via formula (2).

Note that the variational problem (7), (8) might be rewritten in the following equivalent form:

$$\int_0^{t_1} M^2 dt \rightarrow \min. \quad (9)$$

In order to simplify solution to the problem, we introduce the following designation:

$$y(t) = x(t) + \frac{a_0}{a_1}, \quad 0 \leq t \leq t_1, \Leftrightarrow x(t) = y(t) - \frac{a_0}{a_1}, \quad 0 \leq t \leq t_1, \quad (10)$$

where $y(t)$ – the new unknown function. Taking into account the designation (10) we can write the following:

$$\begin{aligned} M &= a_0 + a_1 x + a_2 \ddot{x} + a_3 \overset{IV}{x} + a_4 \overset{VI}{x} = a_1 \left(\frac{a_0}{a_1} + x \right) + a_2 \ddot{x} + a_3 \overset{IV}{x} + a_4 \overset{VI}{x} \\ &= a_1 y + a_2 \ddot{y} + a_3 \overset{IV}{y} + a_4 \overset{VI}{y} = \left[a_1 + a_2 \frac{d^2}{dt^2} + a_3 \frac{d^4}{dt^4} + a_4 \frac{d^6}{dt^6} \right] y. \end{aligned} \quad (11)$$

The condition for the minimum of the functional (9) is the Euler-Poisson equation [14], which in this case may be presented in the following form:

$$\frac{\partial M^2}{\partial y} + \frac{d^2}{dt^2} \frac{\partial M^2}{\partial \ddot{y}} + \frac{d^4}{dt^4} \frac{\partial M^2}{\partial \overset{VI}{y}} + \frac{d^6}{dt^6} \frac{\partial M^2}{\partial \overset{VI}{y}} = 0.$$

By substituting the image (11) into the written equation and using the rule of differentiation of a complex function, we obtain the following:

$$\begin{aligned} 2Ma_1 + \frac{d^2}{dt^2} (2Ma_2) + \frac{d^4}{dt^4} (2Ma_3) + \frac{d^6}{dt^6} (2Ma_4) &= 0 \Leftrightarrow \\ Ma_1 + a_2 \frac{d^2 M}{dt^2} + a_3 \frac{d^4 M}{dt^4} + a_4 \frac{d^6 M}{dt^6} &= 0 \Leftrightarrow \\ \left[a_1 + a_2 \frac{d^2}{dt^2} + a_3 \frac{d^4}{dt^4} + a_4 \frac{d^6}{dt^6} \right]^2 y &= 0. \end{aligned} \quad (12)$$

The obtained equation (12) is a linear, homogeneous differential equation of 12-th order. In order to solve it, we should determine the roots of the characteristic polynomial:

$$Q(\lambda) = \left[a_1 + a_2 \lambda^2 + a_3 \lambda^4 + a_4 \lambda^6 \right]^2.$$

Since the polynomial $Q(\lambda)$ is a square of a polynomial of 6-th order, it has 6 roots of 2-nd order. In order to determine them, we write the following equation:

$$a_1 + a_2 \lambda^2 + a_3 \lambda^4 + a_4 \lambda^6 = 0,$$

in which we introduce the designation: $\lambda^2 = \mu$. As a result, we obtain an algebraic equation of 3-rd order

$$a_1 + a_2 \mu + a_3 \mu^2 + a_4 \mu^3 = 0. \quad (13)$$

Its roots may be determined analytically by using the Cardano's method, or approximately by one of the numerical methods. The solution of the equation (13) depends on the numerical values of the coefficients (5).

If the input parameters of the problem have the following values $m = 5000$ kg, $m_1 = 150$ kg, $I = 30$ kgm², $H = 10$ m, $\omega = 0.075$ rad/s, $r = 0.15$ m, $C = 1.65 \cdot 10^5$ N/m, $V = 0.85$ m/s, $x_0 = 7$ m, $t_1 = 5$ s, $W = 5500$ N, the approximate solutions of equation (13) are $\mu_1 \approx -687.17$, $\mu_2 \approx -3.9041$, $\mu_3 \approx -0.0044954$. The numerical value of W is calculated in the following way: $W = (m + m_1)gq = (5000 + 150) \cdot 9.81 \cdot 0.11 \approx 5500$ N (where q – friction coefficient).

Taking into account the designation $\lambda^2 = \mu$ for the roots of the characteristic polynomial $Q(\lambda)$, we may write:

$$\begin{aligned} \lambda_{1,2} &= \pm \sqrt{\mu_1} \approx \pm i \cdot 26.214 = \pm i \cdot \alpha_1, & \lambda_{3,4} &= \pm \sqrt{\mu_2} \approx \pm i \cdot 1.91759 = \pm i \cdot \alpha_2, \\ \lambda_{5,6} &= \pm \sqrt{\mu_3} \approx \pm 0.067048 = \pm \alpha_3, \end{aligned}$$

where i – imaginary unit.

All the roots $\lambda_{1,2,3,4,5,6}$ of the characteristic polynomial $Q(\lambda)$ are roots of second order. The general solution of the linear homogeneous differential equation (12) is written as follows:

$$y(t) = (C_1 + C_2t) \cos(\alpha_1t) + (C_3 + C_4t) \sin(\alpha_1t) + (C_5 + C_6t) \cos(\alpha_2t) + (C_7 + C_8t) \sin(\alpha_2t) + (C_9 + C_{10}t) e^{\alpha_3t} + (C_{11} + C_{12}t) e^{-\alpha_3t}, \quad 0 \leq t \leq t_1,$$

where $C_{1,\dots,12} = \text{const}$.

Substituting the obtained explicit form of the function $y(t)$ in (10), we obtain the function $x(t)$:

$$x(t) = y(t) - \frac{a_0}{a_1} = (C_1 + C_2t) \cos(\alpha_1t) + (C_3 + C_4t) \sin(\alpha_1t) + (C_5 + C_6t) \cos(\alpha_2t) + (C_7 + C_8t) \sin(\alpha_2t) + (C_9 + C_{10}t) e^{\alpha_3t} + (C_{11} + C_{12}t) e^{-\alpha_3t} - \frac{a_0}{a_1}, \quad 0 \leq t \leq t_1. \quad (14)$$

In order to find the coefficients $C_{1,\dots,12}$, the expression (14) should be substituted into the boundary conditions (8) of the original problem. As a result, we obtain a system of linear algebraic equations. Its approximate solution may be presented as follows: $C_1 \approx -1.3540 \cdot 10^{-6}$, $C_2 \approx 1.0536 \cdot 10^{-7}$, $C_3 \approx 2.09208 \cdot 10^{-8}$, $C_4 \approx 1.8714 \cdot 10^{-7}$, $C_5 \approx 0.036064$, $C_6 \approx -0.014894$, $C_7 \approx 0.020835$, $C_8 \approx -0.003177$, $C_9 \approx -78.196$, $C_{10} \approx 2.9682$, $C_{11} \approx -99.386$, $C_{12} \approx -4.41522$.

Substituting coefficients $C_{1,\dots,12}$ in (14), we obtain the final solution of the variational problem (9).

Then, we should determine the value of $M_{\text{RMS.min}}$. Caring out a proper calculation, we obtain the following value: $M_{\text{RMS.min}} \approx 960.7 \text{ Nm}$.

In order to solve the initial problem (6) we should determine the value $\dot{M}_{\text{RMS.min}}$. It, in turn, requires the determination of the motion law $x = x(t)$, $0 \leq t \leq t_1$, which minimizes the functional:

$$\dot{M}_{\text{RMS.min}} = M_{\text{RMS}}^{(1)} = \left(t_1^{-1} \int_0^{t_1} \dot{M}^2 dt \right)^{1/2} \rightarrow \min, \quad (15)$$

where

$$\dot{M} = a_1 \dot{x} + a_2 \ddot{x} + a_3 \overset{V}{x} + a_4 \overset{VII}{x} = \left[a_1 \frac{d}{dt} + a_2 \frac{d^3}{dt^3} + a_3 \frac{d^5}{dt^5} + a_4 \frac{d^7}{dt^7} \right] x. \quad (16)$$

if the boundary conditions are met:

$$\begin{aligned} t = 0: \quad & x = x_0, \quad \dot{x} = 0, \quad \ddot{x} = x_0 \omega^2, \quad \overset{IV}{x} = 0, \quad \overset{V}{x} = x_0 \omega^4, \quad \overset{VI}{x} = 0, \quad \overset{VII}{x} = x_0 \omega^6, \\ t = t_1: \quad & x = x_0 + \frac{Vt_1}{2}, \quad \dot{x} = V, \quad \ddot{x} = \left(x_0 + \frac{Vt_1}{2} \right) \omega^2, \quad \overset{IV}{x} = 0, \\ & \overset{IV}{x} = \left(x_0 + \frac{Vt_1}{2} \right) \omega^4, \quad \overset{V}{x} = V \omega^4, \quad \overset{VI}{x} = V \omega^6. \end{aligned} \quad (17)$$

As in the case of (8), the boundary conditions (17) ensure elimination of load oscillations. The variational problem (15) may be rewritten in the following equivalent form:

$$\int_0^{t_1} \dot{M}^2 dt \rightarrow \min. \quad (18)$$

The Euler-Poisson equation – the condition for the minimum of the functional (18) – we have presented in the following form:

$$\frac{d}{dt} \frac{\partial \dot{M}^2}{\partial \dot{x}} + \frac{d^3}{dt^3} \frac{\partial \dot{M}^2}{\partial \ddot{x}} + \frac{d^5}{dt^5} \frac{\partial \dot{M}^2}{\partial \overset{V}{x}} + \frac{d^7}{dt^7} \frac{\partial \dot{M}^2}{\partial \overset{VII}{x}} = 0.$$

By using the rule of differentiation of a complex function and substituting the explicit expression (16), we obtain the following:

$$\begin{aligned} \frac{d}{dt} (2Ma_2) + \frac{d^3}{dt^3} (2Ma_2) + \frac{d^5}{dt^5} (2Ma_3) + \frac{d^7}{dt^7} (2Ma_4) &= 0 \Leftrightarrow \\ \frac{dM}{dt} a_1 + a_2 \frac{d^3 M}{dt^3} + a_3 \frac{d^5 M}{dt^5} + a_4 \frac{d^7 M}{dt^7} &= 0 \Leftrightarrow \\ \left[a_1 \frac{d}{dt} + a_2 \frac{d^3}{dt^3} + a_3 \frac{d^5}{dt^5} + a_4 \frac{d^7}{dt^7} \right]^2 x &= 0. \end{aligned} \quad (19)$$

The obtained equation (19) is a linear, homogeneous differential equation of 14-th order. In order to solve it, we should determine the roots of the characteristic polynomial:

$$R(\lambda) = [a_1 \lambda + a_2 \lambda^3 + a_3 \lambda^5 + a_4 \lambda^7]^2 = \lambda^2 [a_1 + a_2 \lambda^2 + a_3 \lambda^4 + a_4 \lambda^6]^2.$$

The polynomial $R(\lambda)$ is a square of a polynomial of the 7-th order. Thus, it has 7 roots of the 2-nd order. One of them is $\lambda_0 = 0$. In order to determine other roots, the following equation must be solved:

$$a_1 + a_2 \lambda^2 + a_3 \lambda^4 + a_4 \lambda^6 = 0.$$

All the roots $\lambda_{0,1,2,3,4,5,6}$ of the characteristic polynomial $R(\lambda)$ are roots of the second order. They lead to the general solution of the linear, homogeneous differential equation (18), which may be written in the following form:

$$\begin{aligned} x(t) &= (C_1 + C_2 t) \cos(\alpha_1 t) + (C_3 + C_4 t) \sin(\alpha_1 t) \\ &+ (C_5 + C_6 t) \cos(\alpha_2 t) + (C_7 + C_8 t) \sin(\alpha_2 t) + (C_9 + C_{10} t) e^{\alpha_3 t} \\ &+ (C_{11} + C_{12} t) e^{-\alpha_3 t} + C_{13} + C_{14} t, \quad 0 \leq t \leq t_1, \end{aligned} \quad (20)$$

where $C_{1,\dots,14} = \text{const.}$

In order to find the coefficients $C_{1,\dots,14}$, the expression (19) should be substituted into the boundary conditions (17) of the original problem. As a result, we will obtain a system of linear algebraic equations. Its approximate solution: $C_1 \approx 0$, $C_2 \approx 0$, $C_3 \approx 0$, $C_4 \approx 0$, $C_5 \approx 0.002602$, $C_6 \approx -0.0031223$, $C_7 \approx 0.027422$, $C_8 \approx -0.0014111$, $C_9 \approx -2279.6$, $C_{10} \approx 34.549$, $C_{11} \approx 6406.3$, $C_{12} \approx 172.48$, $C_{13} \approx -4119.7$, $C_{14} \approx -375.28$. Substituting the determined $C_{1,\dots,14}$ into expression (19) brings the solution of the variational problem (17). Then, we determine the value (15): $\dot{M}_{\text{RMS. min}} \approx 89.4 \text{ Nm/s}$.

The next step is determination of the motion law $x = x(t)$, $0 \leq t \leq t_1$, which minimizes the functional (6) and meets the boundary conditions (17). The coefficient $k > 0$ is included in the first term of the integrand (6) as an adjustment factor. It appears due to the fact that numerical values of $M_{\text{RMS. min}}$ and $\dot{M}_{\text{RMS. min}}$ may significantly differ. Therefore, this additional coefficient has been introduced in order to equalize the influence of the first and the second terms of the integrand (6). The value of k depends on numerical values of $M_{\text{RMS. min}}$ and $\dot{M}_{\text{RMS. min}}$. Solving the corresponding problems, we obtain the following: $M_{\text{RMS. min}} \approx 960.7 \text{ Nm}$ and $\dot{M}_{\text{RMS. min}} \approx 89.4 \text{ Nm/s}$.

In this case, the factor k may be set in the range from 100 to 150. In the frame of the current investigation, it was set to $k = 150$.

The coefficient δ ($0 < \delta < 1$) allows us to control the influence of the torque M and its time derivative \dot{M} on the result of optimization problem (6) solution. Thus, the coefficient δ makes a basis for a compromise between two components of the criterion (6).

In order to simplify further calculations, we introduce the following designation:

$$\delta_1 = \frac{\delta k}{M_{\text{RMS. min}}^2}, \quad \delta_2 = \frac{1 - \delta}{\dot{M}_{\text{RMS. min}}^2}, \quad \delta_{1,2} > 0. \quad (21)$$

Taking into account these expressions, the criterion (6) may be rewritten as follows:

$$K_1 = \left(t_1^{-1} \int_0^{t_1} \delta_1 k M^2 + \delta_2 \dot{M}^2 dt \right)^{1/2} \rightarrow \min. \quad (22)$$

Now, the variational problem (22) may be rewritten in the following equivalent form:

$$t_1 K_1^2 = \int_0^{t_1} \delta_1 M^2 + \delta_2 \dot{M}^2 dt \rightarrow \min. \quad (23)$$

The obtained variational problem (23) is equivalent to the problem (22), which, in turn, is equivalent to the problem (6).

In order to carry out further transformations, we will take into consideration the function:

$$y(t) = x(t) + \frac{a_0}{a_1}, \quad 0 \leq t \leq t_1, \quad \Leftrightarrow \quad x(t) = y(t) - \frac{a_0}{a_1}, \quad 0 \leq t \leq t_1. \quad (24)$$

Note, that $\dot{x} = \dot{y}$, $\ddot{x} = \ddot{y}$ etc.

Taking into account the substitution (24), we may write M and \dot{M} , which are included in the integrand of the criterion (22):

$$\begin{aligned} M &= a_1 y + a_2 \ddot{y} + a_3 \overset{IV}{y} + a_4 \overset{VI}{y} = \left[a_1 + a_2 \frac{d^2}{dt^2} + a_3 \frac{d^4}{dt^4} + a_4 \frac{d^6}{dt^6} \right] y, \\ \dot{M} &= a_1 \dot{y} + a_2 \ddot{\dot{y}} + a_3 \overset{V}{y} + a_4 \overset{VII}{y} = \left[a_1 + a_2 \frac{d^3}{dt^3} + a_3 \frac{d^5}{dt^5} + a_4 \frac{d^7}{dt^7} \right] \frac{d}{dt} y. \end{aligned} \quad (25)$$

In order to solve the problem (23) we write the Euler-Poisson equation:

$$\begin{aligned} \delta_1 \left(\frac{\partial M^2}{\partial y} + \frac{d^2}{dt^2} \frac{\partial M^2}{\partial \ddot{y}} + \frac{d^4}{dt^4} \frac{\partial M^2}{\partial \overset{IV}{y}} + \frac{d^6}{dt^6} \frac{\partial M^2}{\partial \overset{VI}{y}} \right) \\ - \delta_2 \left(\frac{d}{dt} \frac{\partial M^2}{\partial \dot{y}} + \frac{d^3}{dt^3} \frac{\partial M^2}{\partial \ddot{\dot{y}}} + \frac{d^5}{dt^5} \frac{\partial M^2}{\partial \overset{V}{y}} + \frac{d^7}{dt^7} \frac{\partial M^2}{\partial \overset{VII}{y}} \right) = 0. \end{aligned}$$

Which, after calculating all its derivatives, may be rewritten as follows:

$$\begin{aligned} \delta_1 \left[a_1 + a_2 \frac{d^2}{dt^2} + a_3 \frac{d^4}{dt^4} + a_4 \frac{d^6}{dt^6} \right] M \\ - \delta_2 \left[a_1 + a_2 \frac{d^2}{dt^2} + a_3 \frac{d^4}{dt^4} + a_4 \frac{d^6}{dt^6} \right] \frac{d}{dt} \dot{M} = 0. \end{aligned}$$

Substituting the equation (24) into the obtained equation leads to the differential equation:

$$\begin{aligned} \delta_1 \left[a_1 + a_2 \frac{d^2}{dt^2} + a_3 \frac{d^4}{dt^4} + a_4 \frac{d^6}{dt^6} \right] y \\ - \delta_2 \left[a_1 + a_2 \frac{d^2}{dt^2} + a_3 \frac{d^4}{dt^4} + a_4 \frac{d^6}{dt^6} \right] \frac{d^2}{dt^2} y = 0, \end{aligned}$$

or finally

$$\left[a_1 + a_2 \frac{d^2}{dt^2} + a_3 \frac{d^4}{dt^4} + a_4 \frac{d^6}{dt^6} \right]^2 \left(\delta_1 - \delta_2 \frac{d^2}{dt^2} \right) y = 0, \quad 0 < t < t_1. \quad (26)$$

Equation (26) is a linear, homogeneous ordinary differential equation. In order to find its solution, it is necessary to determine the roots of a characteristic equation, which has the following form:

$$P(\lambda) = (a_1 + a_2\lambda^2 + a_3\lambda^4 + a_4\lambda^6)^2 (\delta_1 - \delta_2\lambda^2) = 0.$$

It may be divided into two equations:

$$a_1 + a_2\lambda^2 + a_3\lambda^4 + a_4\lambda^6 = 0, \quad \delta_1 - \delta_2\lambda^2 = 0. \quad (27)$$

The coefficients of the first equation (27) depend on the numerical parameters of the problem and do not depend on the factor k and the weight coefficient δ . The equation is solved in the first variational problem while determining the minimum of the RMS value of the drive torque. The results may be presented as follows:

$$\begin{aligned} \lambda_{1,2} &= \pm\sqrt{\mu_1} \approx \pm i26.214 = \pm i\alpha_1, \\ \lambda_{3,4} &= \pm\sqrt{\mu_2} \approx \pm i1.9759 = \pm i\alpha_2, \\ \lambda_{5,6} &= \pm\sqrt{\mu_3} \approx \pm i0.067048 = \pm i\alpha_3. \end{aligned} \quad (28)$$

Since $\delta_{1,2} > 0$, the second equation of the system (27) has two obvious real solutions:

$$\lambda = \lambda_{7,8} = \pm\sqrt{\frac{\delta_1}{\delta_2}}. \quad (29)$$

The numerical values of λ depend on the parameters of the problem, the values of the factor k and coefficient δ . The solutions (29) define two more roots of the characteristic polynomial $P(\lambda)$.

Thus, the combination of solutions (27) and (29) brings the roots of $P(\lambda)$ (28), (29). Then, the general solution of equation (26) may be written as follows:

$$\begin{aligned} y(t) &= (C_1 + C_2t) \cos(\alpha_1t) + (C_3 + C_4t) \sin(\alpha_1t) \\ &+ (C_5 + C_6t) \cos(\alpha_2t) + (C_7 + C_8t) \sin(\alpha_2t) + (C_9 + C_{10}t) e^{\alpha_3t} \\ &+ (C_{11} + C_{12}t) e^{-\alpha_3t} + C_{13}e^{\sqrt{\frac{\delta_1}{\delta_2}}t} + C_{13}e^{-\sqrt{\frac{\delta_1}{\delta_2}}t}, \quad 0 \leq t \leq t_1, \end{aligned}$$

where $C_{1,\dots,14} = \text{const}$. If we substitute the determined function $y(t)$ into expression (24), we obtain an explicit form for the desired solution to the variational problem (23):

$$\begin{aligned} x(t) &= y(t) - \frac{a_0}{a_1} = (C_1 + C_2t) \cos(\alpha_1t) + (C_3 + C_4t) \sin(\alpha_1t) \\ &+ (C_5 + C_6t) \cos(\alpha_2t) + (C_7 + C_8t) \sin(\alpha_2t) + (C_9 + C_{10}t) e^{\alpha_3t} \\ &+ (C_{11} + C_{12}t) e^{-\alpha_3t} + C_{13}e^{\sqrt{\frac{\delta_1}{\delta_2}}t} + C_{13}e^{-\sqrt{\frac{\delta_1}{\delta_2}}t}, \quad 0 \leq t \leq t_1. \end{aligned} \quad (30)$$

In order to determine the unknown constants $C_{1,\dots,14}$, we substitute (30) into the boundary conditions (17) and obtain a system of linear algebraic equations with respect to the constants $C_{1,\dots,14}$. The solution of these equations leads to the final solution of the problem (23). The obtained solution allows us to determine all the motion characteristics of the trolley movement mechanism. The solution is valid for different values of the coefficient $\delta \in (0, 1)$. One may choose what is more important in the optimal control law (minimization of torque RMS or torque derivative RMS) by tuning the numerical value of δ : the greater the value, the greater the impact of the first term (9), and vice versa.

Let $\delta = 0.9$. In this case, the solution (30) will have the following form:

$$\begin{aligned}
 x = x(t) = & 184.5 + (C_1 + C_2t) \cos(26.21t) + (C_3 + C_4t) \sin(26.21t) \\
 & + (C_5 + C_6t) \cos(1.976t) + (C_7 + C_8t) \sin(1.976t) + e^{0.06705} (C_9 + C_{10}t) \\
 & + e^{-0.06705} (C_{11} + C_{12}t) + C_{13}e^{3.421t} + C_{14}e^{-3.421t}, \quad 0 \leq t \leq t_1,
 \end{aligned}$$

where $C_1 \approx 0$, $C_2 \approx 0$, $C_3 \approx 0$, $C_4 \approx 0$, $C_5 \approx 0.029660$, $C_6 \approx -0.01418$, $C_7 \approx 0.04086$, $C_8 \approx -3.339 \cdot 10^{-3}$, $C_9 \approx -77.58$, $C_{10} \approx 2.988$, $C_{11} \approx -99.99$, $C_{12} \approx -4.571$, $C_{13} \approx 0$, $C_{14} \approx -4.014 \cdot 10^{-3}$.

4. Results and discussion

As a result of the conducted research, we have built graphical dependencies of the kinematic (Figs. 2–7), power (Figs. 8, 9), and energy (Fig. 10) characteristics of the trolley movement mechanism during steady slewing of the tower crane. The mentioned plots have been determined for three optimal modes of motion: (14), (20), and (30). In Figs. 2–10, the continuous lines refer to criterion (6); the dashed lines refer to criterion (7); the dotted lines refer to criterion (15).

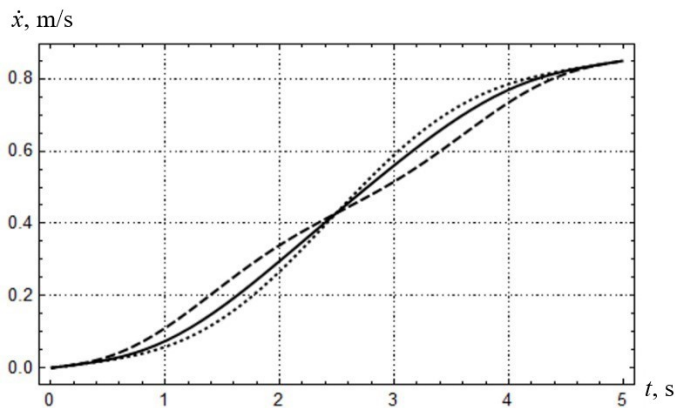


Fig. 2. Plots of the load velocity

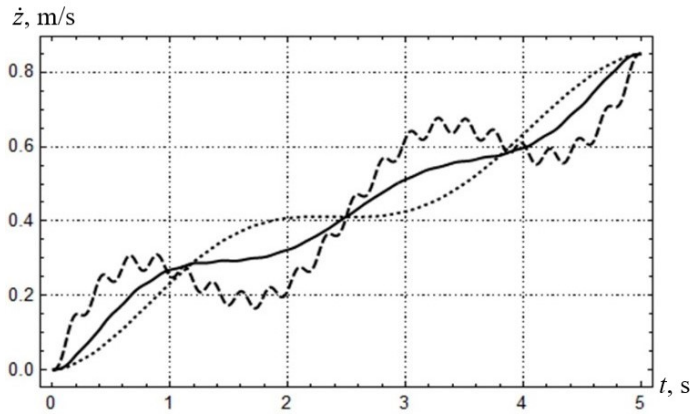


Fig. 3. Plots of the trolley velocity

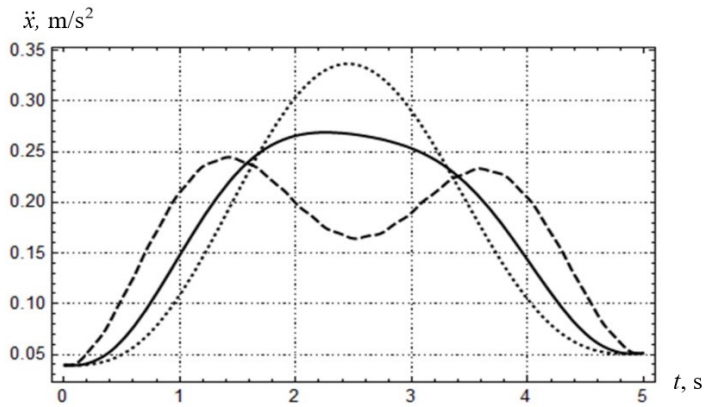


Fig. 4. Plots of the load acceleration

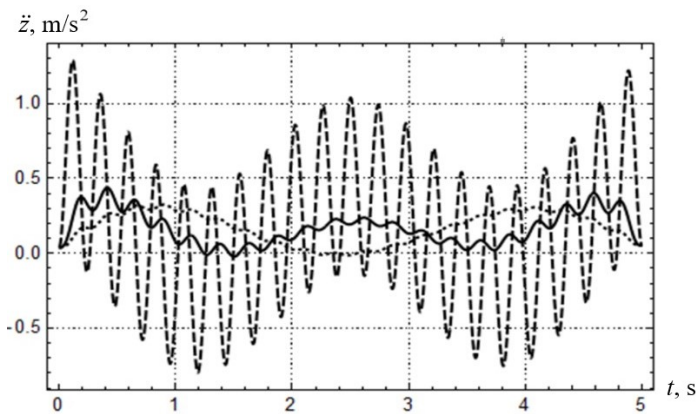


Fig. 5. Plots of the trolley acceleration

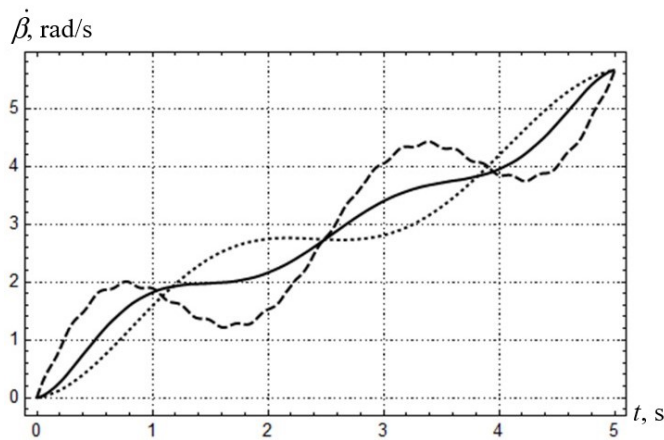


Fig. 6. Plots of the drum angular velocity

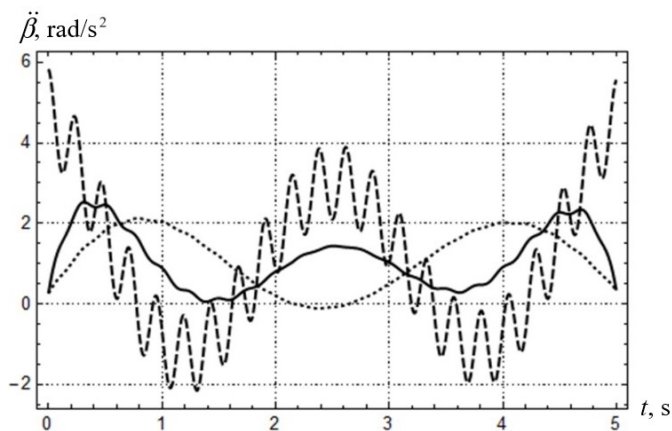


Fig. 7. Plots of the drum angular acceleration

The analysis of the load movement (Fig. 2) for all of the criteria (6), (7), (15) shows that the course of its velocity is smooth. In opposite, the trolley (Fig. 3) and the drum (Fig. 6) exhibit low-frequency oscillations. These are caused by the pendulum oscillations of the load. The oscillations are eliminated during the optimal start of the system (indeed, velocities and positions (not shown) of the load and trolley are the same). In addition, during the motion in an optimal mode, significant high-frequency oscillations of the trolley and the drum might be observed. This applies to the optimization by the (7) criterion. At the same time, one also observes the largest amplitudes of low-frequency oscillations of the trolley and the drum.

Almost the same character of the trolley movement is observed for the modes of motion optimal according to the criteria (15) and (6). The same may be said about the drum movement.

However, there is a variety of amplitudes of the load acceleration: the maximum (0.34 m/s^2) refers to the mode of motion optimal with criterion (15); the value 0.27 m/s^2 – is the maximum of load acceleration for mode of motion optimal according to criterion (6); the lowest (0.24 m/s^2) value refers to the mode optimal with criterion (7).

The courses of acceleration of the trolley and the drum that are optimal according to criterion (15) show an almost smooth behavior. We note only a minor low-frequency oscillation component. The trolley and the drum accelerations, which are obtained with criterion (7), have significant low- and high-frequency oscillations. The maximum values of the trolley and the drum acceleration are 1.4 m/s^2 and 5.75 rad/s^2 , respectively. For comparison, the values of these indicators obtained with optimization criterion (6) are 0.40 m/s^2 and 2.5 rad/s^2 , respectively, and with criterion (15) they are 0.32 m/s^2 and 2.10 rad/s^2 , respectively.

The analysis of traction force in the rope in the mode of motion optimal according to criterion (7) (Fig. 8) indicates that there appear both low- and high-frequency oscillations. The maximum value of the traction force for this mode is the smallest one, and equals 6640 N . The course of traction force in the mode of motion optimal according to criterion (15) is smooth. However, the force reaches the maximum value of 6900 N . The mode of motion optimal according to the criterion (6) is characterized by the maximum value of the traction force 6650 N . The course of the force is almost smooth, with minor high-frequency oscillations. This example shows that by using optimization criterion (6), one may obtain a compromise between the maximum value of the rope traction force and a reduction or complete elimination of high-frequency oscillations in the elements of the trolley movement mechanism.

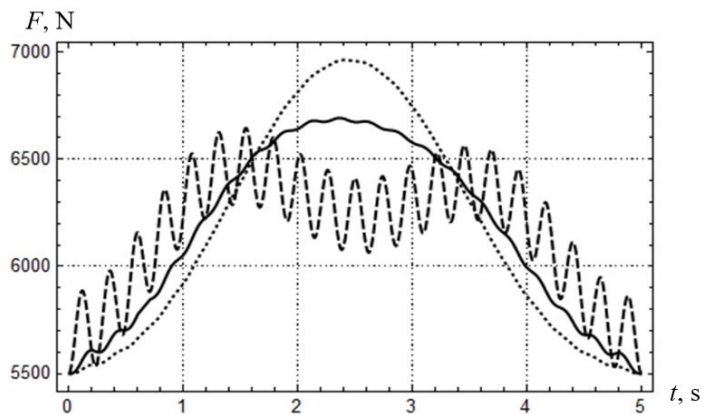


Fig. 8. Plots of the traction force in the rope

The maximum values of the drive torque for all of the optimal modes of motion (Fig. 9) differ insignificantly in the range from 1025 N to 1040 N . However, for the mode of motion optimal according to criterion (7), one observes low-frequency

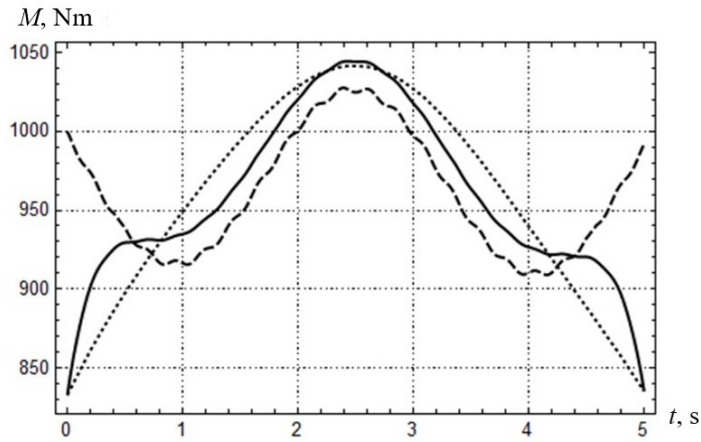


Fig. 9. Plots of the drive torque

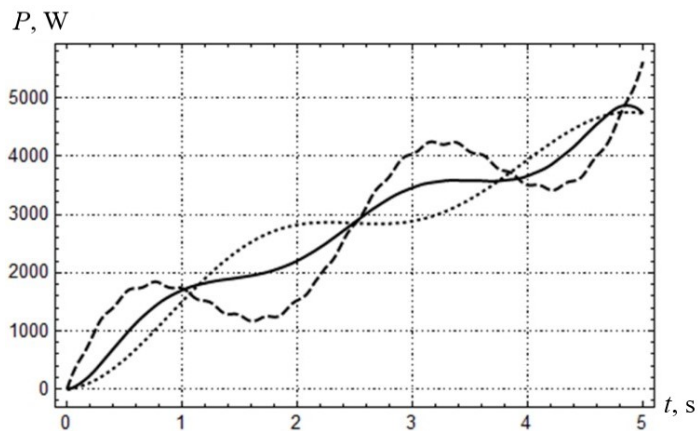


Fig. 10. Plots of the drive power

oscillations. At the very first moment of the start, there is a discontinuity between the drive torque and the torque, which refers to the force W . This effect may cause high-frequency oscillations in the drive components and in the metal structure of the crane. The mentioned effect is absent in the other two optimal modes of motion, where the drive torque changes smoothly without oscillations.

Fig. 10 indicates that, in all of the optimal modes of motion, the drive power changes with low-frequency oscillations. However, in the mode of motion optimal according to criterion (7) the amplitude of these oscillations is the largest, and there is also a small high-frequency component. The overall maximum value (maximal value among the three variational problems) of power (5700 W) refers to this optimization criterion, as well. The lowest value of power (4750 W) refers to criterion (15). The maximum value of power when criterion (6) is applied equals 4850 W.

5. Conclusions

The article presents the results of research on the trolley movement mechanism optimization. The trolley accelerates from the rest state to a steady velocity and the tower slews at a steady angular velocity. Three variational problems, which refer to the optimization problems, have been formulated and solved. In these problems, RMS values of the drive torque, its rate, and the combination of these indicators have been taken as the criteria for minimization. The solutions to all three variational problems have been reduced to analytical dependencies that describe optimal modes of the system motion.

The advantages and disadvantages of each of the modes of motion associated with individual optimization criteria have been described. The force loads in the traction element of the trolley and the drive mechanism have been reduced. This result refers to the mode of the system motion optimal according to criterion (7) (the first variational problem). However, in this case there are significant low- and high-frequency oscillations of the drive elements and the metal structure of the boom system, as well as high energy consumption.

The maximum values of force and kinematic indicators, which refer to the solution of the second variational problem (that refers to criterion (15)), are slightly increased, in comparison with the first one. However, the trolley movement mechanism increases the smoothness of the motion and low-frequency (pendulum) load oscillations are completely eliminated.

In the third variational problem (criterion (6)), a compromise between the two previously-mentioned modes has been obtained. As a result, a reasonable level of the force loads in the system elements has been obtained. Additionally, the compromise approach allowed for decreasing high-frequency oscillations of the trolley, drum, and other elements of the system. Indeed, the reasonable selection of the weight coefficient in a complex criterion leads to the almost complete elimination of high-frequency oscillations of the trolley movement mechanism. However, some of the maximum values of kinematic and force characteristics slightly increase in comparison with the results that are obtained for the first and the second variational problem.

Taking into account all the advantages and disadvantages of the optimal modes of motion we may recommend application of the mode of motion optimal according to the complex criterion (6).

In order to implement the proposed optimal control law in practice, frequency inverters, microcontrollers and proper sensors should be used. It is desirable to consider frequency inverters for crane drives. In calculation of the optimal law of motion, one must rely on the measured values of load mass m , initial trolley position x_0 , and length of the cable H . For the measurement of m , a tension sensor may be used (it measures the tension of the cable), determination of values x_0 and H needs optical encoders. In the software of the optimal control system, all the

measured values are used to recalculate the optimal control law formulae according to the current m , H , and x_0 values.

References

- [1] Y. Qian and Y. Fang. Switching logic-based nonlinear feedback control of offshore ship-mounted tower cranes: a disturbance observer-based approach. *IEEE Transactions on Automation Science and Engineering*, 16(3):1125–1136, 2018. doi: [10.1109/TASE.2018.2872621](https://doi.org/10.1109/TASE.2018.2872621).
- [2] M. Zhang, Y. Zhang, B. Ji, C. Ma, and X. Cheng. Modeling and energy-based sway reduction control for tower crane systems with double-pendulum and spherical-pendulum effects. *Measurement and Control*, 53(1-2):141–150, 2020. doi: [10.1177/0020294019877492](https://doi.org/10.1177/0020294019877492).
- [3] M. Zhang, Y. Zhang, H. Ouyang, C. Ma, and X. Cheng. Adaptive integral sliding mode control with payload sway reduction for 4-DOF tower crane systems. *Nonlinear Dynamics*, 99(7):2727–2741, 2020. doi: [10.1007/s11071-020-05471-3](https://doi.org/10.1007/s11071-020-05471-3).
- [4] T. Yang, N. Sun, H. Chen, and Y. Fang. Observer-based nonlinear control for tower cranes suffering from uncertain friction and actuator constraints with experimental verification. *IEEE Transactions on Industrial Electronics*, 68(7):6192–6204, 2021. doi: [10.1109/TIE.2020.2992972](https://doi.org/10.1109/TIE.2020.2992972).
- [5] J. Peng, J. Huang, and W. Singhose. Payload twisting dynamics and oscillation suppression of tower cranes during slewing motions. *Nonlinear Dynamics*, 98:1041–1048, 2019. doi: [10.1007/s11071-019-05247-4](https://doi.org/10.1007/s11071-019-05247-4).
- [6] S. Fasih, Z. Mohamed, A. Husain, L. Ramli, A. Abdullahi, and W. Anjum. Payload swing control of a tower crane using a neural network-based input shaper. *Measurement and Control*, 53(7-8):1171–1182, 2020. doi: [10.1177/0020294020920895](https://doi.org/10.1177/0020294020920895).
- [7] D. Kruk and M. Sulowicz. AHRS based anti-sway tower crane controller. *2019 20th International Conference on Research and Education in Mechatronics (REM)*, 2019. doi: [10.1109/rem.2019.8744117](https://doi.org/10.1109/rem.2019.8744117).
- [8] R.E. Samin and Z. Mohamed. Comparative assessment of anti-sway control strategy for tower crane system. *AIP Conference Proceedings*, 1883:020035, 2017. doi: [10.1063/1.5002053](https://doi.org/10.1063/1.5002053).
- [9] S.-J. Kimmerle, M. Gerdt, and R. Herzog. Optimal control of an elastic crane-trolley-load system – a case study for optimal control of coupled ODE-PDE systems – (extended version with two appendices). *Mathematical and Computer Modelling of Dynamical Systems*, 24(2):182–206, 2018. doi: [10.1080/13873954.2017.1405046](https://doi.org/10.1080/13873954.2017.1405046).
- [10] V. Loveikin, Y. Romasevych, I. Kadykalo, and A. Liashko. Optimization of the swinging mode of the boom crane upon a complex integral criterion. *Journal of Theoretical and Applied Mechanics*, 49(3):285–296, 2019. doi: [10.7546/JTAM.49.19.03.07](https://doi.org/10.7546/JTAM.49.19.03.07).
- [11] Z. Liu, T. Yang, N. Sun, and Y. Fang. An antiswing trajectory planning method with state constraints for 4-DOF tower cranes: design and experiments. *IEEE Access*, 7:62142–62151, 2019. doi: [10.1109/ACCESS.2019.2915999](https://doi.org/10.1109/ACCESS.2019.2915999).
- [12] M. Böck and A. Kugi. Real-time nonlinear model predictive path-following control of a laboratory tower crane. *IEEE Transactions on Control System Technology*, 22(4):1461–1473, 2014. doi: [10.1109/TCST.2013.2280464](https://doi.org/10.1109/TCST.2013.2280464).
- [13] Š. Ileš, J. Matuško, and F. Kolonić. Sequential distributed predictive control of a 3D tower crane. *Control Engineering Practice*. 79:22–35, 2018. doi: [10.1016/j.conengprac.2018.07.001](https://doi.org/10.1016/j.conengprac.2018.07.001).
- [14] K.W. Cassel. *Variational Methods with Applications in Science and Engineering*. Cambridge University Press, 2013. doi: [10.1017/CBO9781139136860](https://doi.org/10.1017/CBO9781139136860).